

# Characterization of thermal rectification in asymmetrical-structured materials with inhomogeneous mass distribution

M. Romero-Bastida and F. Tejada-Méndez  
*Sección de Estudios de Posgrado e Investigación Escuela Superior de  
Ingeniería Mecánica y Eléctrica-Culhuacán,  
Instituto Politécnico Nacional,  
Avenida Santa Ana 1000, Colonia San Francisco Culhuacán,  
Delegación Coyoacán, Distrito Federal 04430, Mexico.  
e-mail: mromerob@ipn.mx*

Received 6 April 2015; accepted 29 October 2015

We study the asymmetrical heat flux present in a one-dimensional, two-segment, nearest-neighbor anharmonic oscillator system subjected to the influence of a temperature gradient for two different mass distributions. For a small system size the largest asymmetry in the heat flux is obtained for the case wherein one segment has larger mass values than the other one, the lowest with the already considered uniform mass distribution, and an intermediate one with a linear mass gradient along the system length. These results are also obtained in the largest system size limit, wherewith it was observed that the heat flux increases as the system size does so for the case of the two segments with dissimilar mass value.

*Keywords:* Low-dimensional asymmetric heat conduction; nonlinear dynamical systems

En este trabajo estudiamos el flujo de calor asimétrico presente en un sistema unidimensional de osciladores anarmónicos acoplados a primeros vecinos, compuesto de dos segmentos diferentes y sujeto a la influencia de un gradiente de temperatura para el caso de dos distribuciones de masa distintas. Para tamaños de sistema pequeños la mayor asimetría en el flujo de calor se obtiene para el caso en el cual uno de los segmentos tiene mayor masa que el otro, la menor para el caso ya conocido de masa uniforme y un caso intermedio para un gradiente de masa a lo largo de toda la longitud del sistema. Estos resultados se mantienen para tamaños de sistema grandes, con los cuales se observa que el flujo de calor se incrementa conforme también lo hace el tamaño del sistema para el caso de los dos segmentos con diferente masa.

*Descriptores:* Conducción de calor asimétrica de baja dimensionalidad; sistemas dinámicos no-lineales

PACS: 44.10.+i, 05.60.-k, 05.70.Ln

## 1. Introduction

Thermal rectification, *i.e.* asymmetrical heat flux, has been a rapidly growing research field in the last decade [1]. Although it was experimentally discovered a long time ago [2], it was only when the first computer simulation results of a rectifying device, modeled by three coupled one-dimensional anharmonic oscillator lattices with different parameters in each segment, were obtained that the field began to make substantial progress [3]. After this first successful implementation, which had a rectification efficiency (defined as the ratio of the thermal fluxes in two opposite directions, see below) of only a factor of 2, a rise to a factor about 100–200 was achieved by coupling two oscillator chains interacting with a substrate described by a Frenkel-Kontorova (FK) on-site potential [4] and even about 2000 in a latter work [5]. These results attracted increasing attention due to its important potential-energy-saving applications in recent years [6]. Furthermore, models of a thermal transistor [7], logic gates [8], and even thermal memories [9], which provide the possibility to design a “phononic computer,” have been proposed. However, there are several problems to be resolved in the so-far proposed models before the aforementioned proposals can be experimentally implemented; there-

fore, a more in-depth understanding of the asymmetric heat conduction is needed and has indeed been pursued. See Ref. 10 for a recent review.

Despite the success so far achieved in the field, it has been noted that the rectification effect of the heat flux as reported in Refs. 3 to 5, and 11 for the three- and two-segment models is possible only in the weak interfacial coupling limit [12, 13]. Therefore, the performance of a thermal device built on such principle depends critically on the properties of the interface, which are very difficult to control in practice [14], resulting in a poor reproducibility of the measurements of the thermal boundary resistance. As a consequence, the functionality of such thermal device can be quite unpredictable due to insufficient information about atomic interfacial conditions. Nevertheless, it is known that, in the thermodynamic limit, the heat conduction of two-segment lattices is determined only by the heat transport properties of the segments and is independent of the interface properties and system size; therefore, by selecting materials with the proper properties a thermal rectifier can be build [15]. These ideas were successfully used to develop the first model of a thermal rectifier that works in the thermodynamic limit by coupling two different anharmonic lattices: a FK, which has a thermal conductivity that increases as a function of temperature, and a  $\Phi^4$  lattice, which

has an opposite behavior [16]. The operation of this device can be easily understood from the basic laws of heat conduction as follows: when the extreme of the lattice corresponding to the segment described by the FK potential is kept at a higher temperature than the opposite extreme, which corresponds to that defined by the  $\Phi^4$  potential, the sample has on average a high thermal conductivity, and so there is a significant thermal flux; if the boundary conditions are reversed the total thermal conductivity of the entire sample is lower than in the former case for these conditions, thus leading to a diminished thermal flux. Following this proposal it has been possible to experimentally construct thermal rectifiers of macroscopic size that work both in the low [17] and high [18] temperature regime; the former is made of two perovskite cobalt oxides ( $\text{LaCoO}_3$  and  $\text{La}_{0.7}\text{Sr}_{0.3}\text{CoO}_3$ , the former being an insulator of well-ordered structure and the latter a disordered metal) and the latter of two aluminium-based alloys ( $\text{Al}_{72.6}\text{Re}_{17.4}\text{Si}_{10}$  and  $\text{Al}_{71.6}\text{Mn}_{17.4}\text{Si}_{11}$ ). Despite this undeniable success, the rectification efficiency of these devices is very low, which highlights the importance of exploring further mechanisms to enhance the rectification effect.

Within the realm of the mesoscopic dimensions the first successful experimental implementation of a thermal rectifier by deposition of amorphous  $\text{C}_6\text{H}_{16}\text{Pt}$  [19] on a single side of both single-walled and multi-walled carbon nanotubes (CNs) inspired various theoretical works that aimed to explore the mechanism responsible of the studied effect [20–23]. In particular, it was determined in Ref. 20 that a nearest-neighbor anharmonic lattice with an asymmetrical mass loading along its length can properly work as a rectifying device. The mechanism responsible of the rectification in this system can be explained as follows: when the heavy mass-loaded end is at a higher temperature than the light mass end of the lattice the energy spectrum of two given oscillators on each side overlap in the low frequency region and thus the heat can easily flow in the direction of the temperature gradient. For reversed boundary conditions, *i.e.* when the light mass end is at a higher temperature than the heavy mass end, there is a mismatch of the aforementioned spectra and thus the heat flux is hindered, notwithstanding the existence of a temperature gradient. This temperature-dependent phonon spectra shift is a purely anharmonic effect, and therefore in the harmonic mass-graded lattice, although it presents heat conduction—which is absent in the homogeneous mass harmonic lattice [24]—, there is no rectification altogether [20].

The aforementioned rectification mechanisms, *i.e.* asymmetric mass-loading and dissimilar thermal conductivity dependence on temperature, are the most predominant ones in nanostructured materials [1]. Now, as far as we are aware of, there has been no effort whatsoever to explore the possibility of implementing two different rectifying mechanisms in the same system to determine if they can work constructively to enhance its rectification efficiency. Since it has been difficult make the rectification factor reach one order of magnitude, which is an arbitrary limit required to deem the effect useful in engineering applications—specially in the nano and meso-

scopic dimensions—, the aforementioned suggestion offers the possibility to increase in an easy way the rectification efficiency of a system that works with a bulk mechanism (dissimilar thermal conductivity dependence on temperature for different spatial regions of the sample) by the inclusion of an additional molecular mechanism (asymmetric mass-loading). If positive, this proposal could have a significant impact by increasing the feasibility, not only of the already mentioned thermal logic gates and memories [7–9], but as well of thermal energy harvesting and other heat control devices. Thus, in this work we propose to explore the feasibility of including two different rectification mechanisms by characterizing the rectifying behavior of the two-segment model system considered in Ref. 16 with two different mass distributions: the first one corresponds to a linear mass-gradient considered in previous theoretical studies [20, 22, 23], and the other is a completely asymmetric one, with different mass loadings in the two segments composing the system. It is important to notice that this latter mass distribution, which has not been considered in the theoretical work so far performed, is indeed closer to the original experimental implementation of the mass-loaded CN [19]. Furthermore, this mass distribution is much easier to achieve experimentally than the linear mass-gradient so far considered.

The plan of this work is as follows: in Sec. 2 we present the model as well as our methodology. Results for both small and large system sizes are reported in Sec. 3. Finally, in Sec. 4 we discuss the results so far obtained and propose other ways to further improve them.

## 2. model and methodology

The herein considered one-dimensional system consists of two different nearest-neighbor lattices, each consisting of  $N/2$  oscillators. The Hamiltonian of the entire system can be written, in terms of dimensionless variables, as

$$H_{FK+\Phi^4} = \sum_{i=1}^{N/2} \left( \frac{p_i^2}{2m_i} + \frac{1}{2}(q_{i+1} - q_i)^2 + \beta(1 - \cos q_i) \right) + \sum_{i=N/2+1}^N \left( \frac{p_i^2}{2m_i} + \frac{1}{2}(q_{i+1} - q_i)^2 + \frac{\alpha}{2}q_i^2 + \frac{\alpha}{4}q_i^4 \right), \quad (1)$$

where  $p_i$  is the momentum of the  $i$ th oscillator,  $q_i$  its corresponding displacement from the equilibrium position, and  $m_i$  the inertial mass. The constants  $\alpha$  and  $\beta$  quantify the amplitude of the specific on-site potential for each segment and thus define the considered models;  $\beta$  corresponds to the FK model, being the first segment of the system, and  $\alpha$  to the  $\Phi^4$  model, being the second one.

The equations of motion for the above defined system, when coupled to two stochastic thermal reservoirs operating at different temperatures, are  $\dot{q}_i = p_i/m_i$  and

$$\begin{aligned}
\dot{p}_i &= F(q_i - q_{i-1}) - F(q_{i+1} - q_i) - \partial_{q_i} U_{FK,\Phi^4}(q_i) \\
&+ \sum_{j=1}^{n_L} \left( \xi_L^{(j)} - \gamma_L p_i \right) \delta_{ij} \\
&+ \sum_{k=N-n_R+1}^N \left( \xi_R^{(k)} - \gamma_R p_i \right) \delta_{ik}, \quad (2)
\end{aligned}$$

with  $F(x) = -\partial_x V(x)$  and  $\xi_{L/R}^{(i)}$  being random forces drawn from a Gaussian distribution with zero mean and a variance that obeys the fluctuation-dissipation relation  $\langle \xi_{L,R}^{(i)}(t) \xi_{L,R}^{(k)}(t') \rangle = 2\gamma_{L,R} T_{L,R} m_i \delta_{ik} \delta(t-t')$ . The friction coefficients  $\gamma_{L,R}$  quantify the interaction of each thermal reservoir with the oscillator lattice,  $n_{L,R}$  are the number of oscillators at the extremes of the lattice connected to the thermal reservoirs operating at temperatures  $T_L$  and  $T_R$ , respectively. In all simulations hereafter reported we employ the values  $n_{L,R} = 2$  and  $\gamma_{L,R} = 0.1$ , together with fixed boundary conditions ( $q_0 = q_{N+1} = 0$ ). The above equations of motion were integrated employing a stochastic velocity-Verlet algorithm with a timestep of  $\Delta t = 0.01$  [25]; total integration time was of  $10^6 - 10^7$  time units.

The local heat flux  $J(x, t)$  is computed as

$$J(x, t) = \frac{1}{N} \sum_i j_i \delta(x - x_i),$$

where  $x_i = q_i + ia$  is the position of the  $i$ th oscillator,  $a$  is the lattice constant (taken as  $a = 1$  hereafter), and

$$j_i = \frac{1}{2} (\dot{x}_{i+1} + \dot{x}_i) F(x_{i+1} - x_i) + \dot{x}_i h_i, \quad (3)$$

where

$$\begin{aligned}
h_i &= \frac{p_i^2}{2m_i} + U_{FK,\Phi^4}(q_i) \\
&+ \frac{1}{2} [V(q_{i+1} - q_i) + V(q_i - q_{i-1})] \quad (4)
\end{aligned}$$

denotes the local energy density at the  $i$ th site. After a transient time the heat flux becomes independent of the position, *i.e.*  $J(x, t) \rightarrow J(t)$ ; therefore the total heat flux is computed as  $J = \langle J(t) \rangle_t$ , being  $\langle \dots \rangle_t$  a temporal average. If  $T_L > T_R$  the resulting flux is denoted as  $J_+$ , but if  $T_L < T_R$  as  $J_-$ . The system works as a thermal rectifier if  $|J_+| > |J_-|$ . Then the relation  $r \equiv |J_+ / J_-|$  quantifies the rectification efficiency of the system;  $r \rightarrow 1$  corresponds to absence of rectification, whereas if  $r \rightarrow \infty$  holds, then perfect rectification is obtained.

### 3. Results

Our first result corresponds to the effect of the temperature difference  $\Delta T = T_L - T_R$  on thermal rectification  $r$  for an equal-mass system, *i.e.*  $m_i = 1 \forall i$ . We choose a system size

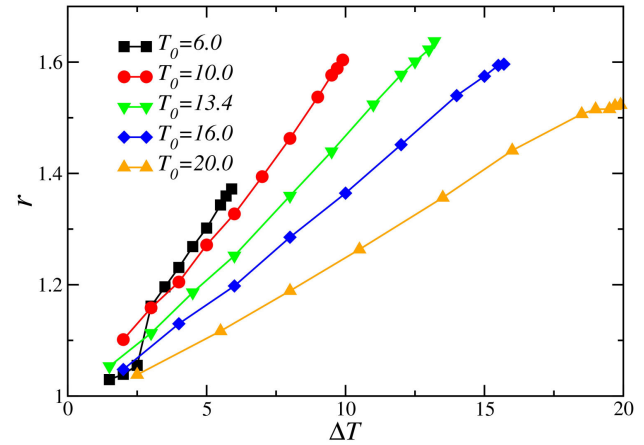


FIGURE 1. (Color online) Thermal rectification  $r$  vs  $\Delta T$  for the homogeneous-mass case and different  $T_0$  values. System size of  $N = 128$ , with  $\beta = 1.5$  and  $\alpha = 0.02$ .

of  $N = 128$  with values of  $k = 1$ ,  $\beta = 1.5$ , and  $\alpha = 0.02$  for the constants that define the system. The reservoir temperatures are taken as  $T_{L,R} = T_0 \pm \Delta T$ , being  $T_0$  the average system temperature. Figure 1 displays  $r$  vs  $\Delta T$  for values of the average temperature of  $T_0 = 6.0, 10.0, 13.4, 16.0,$  and  $20.0$ . It is clear that  $r$  grows as  $\Delta T$  increases with an approximately linear dependence of the former on the latter. It can also be observed that the rate of increase of  $r$  decreases as the average temperature increases. Our results are consistent with those already reported in the literature [16], thus corroborating the validity of our implementation of the model.

The second case to be considered is that of a system with a linear mass gradient along its length which has already been considered in previous works [20, 22, 23]. The mass of the  $i$ th oscillator is given by  $m_i = M_{\max} - (i-1)(M_{\max} - M_{\min}) / (N-1)$ .  $M_{\max}$  and  $M_{\min}$  are the mass of the oscillators at the left and right ends, respectively. In the following we always take  $M_{\min} = 1$ . In Fig. 2 we present the result of

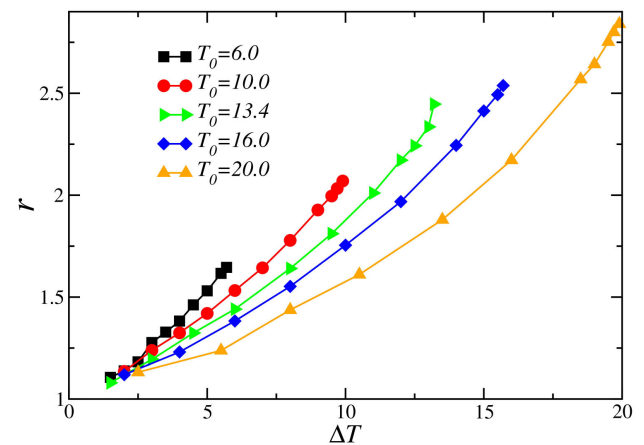


FIGURE 2. (Color online) Thermal rectification  $r$  vs  $\Delta T$  for the mass-graded case with  $M_{\max} = 10$  for different  $T_0$  values. Same  $N$ ,  $\beta$ , and  $\alpha$  values as in Fig. 1.

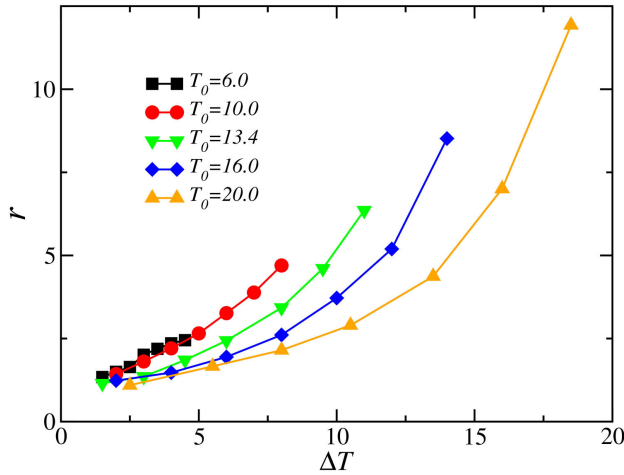


FIGURE 3. (Color online) Thermal rectification  $r$  vs  $\Delta T$  for the case wherein the two segments have dissimilar masses (see text for explanation) for various  $T_0$  values. Same  $N$ ,  $\beta$ , and  $\alpha$  values as in Fig. 1.

the dependence of thermal rectification with respect to  $\Delta T$  for the same  $T_0$  values than in Fig. 1, but now for the case of a mass gradient of  $M_{\max} = 10$ , with the left reservoir connected to  $M_{\max}$  and the right one to  $M_{\min}$ . It can be readily appreciated that, as  $T_0$  increases, the linear dependence of  $r$  on  $\Delta T$  observed in Fig. 1 changes to an exponential-like one. Furthermore, a significant increase in thermal rectification is observed for the same  $\Delta T$  values compared to the former case, *i.e.*  $r(\Delta T \sim 20) \sim 1.5$  for the homogeneous, unitary-mass case, whereas for the mass-graded lattice  $r(\Delta T \sim 20) \sim 2.5$ . Similar increments in rectification when a mass-gradient is present have been previously reported for similar systems [20, 22]. It is important to mention that the election of the direction of the mass-gradient is critical to the performance of this device. In our study the side corresponding to the FK lattice has the greatest mass-loading. If the direction of the mass-gradient is reversed we obtain  $r(\Delta T \sim 20) \sim 0.7$ , *i.e.* rectification diminishes. This reduction can be explained because the phonon spectra of the heavy end is located in the low frequency region [20], which favors the heat flux and thus diminishes the overall rectification of the system.

The next considered case corresponds to a system wherein the mass of each segment is different. In Fig. 3 we display the results for a mass distribution of  $m_i = 10 \forall i = 1, \dots, N/2$  and  $m_i = 1 \forall i = N/2 + 1, \dots, N$ . Further differences with the aforementioned cases can be noted. The exponential dependence of  $r$  on  $\Delta T$  already observed for the mass-graded case is greatly increased, with an ensuing increment in rectification for all  $T_0$  values employed. In particular, for  $\Delta T \sim 20$  we obtain  $r \sim 12.5$ , which is significantly higher than the corresponding values of  $r = 1.5$  for the homogeneous, unitary-mass case and 2.5 for the mass-graded lattice. Therefore, for constant  $N$  it is clear that an increase in the mass-loading asymmetry affords the highest rectification figure.

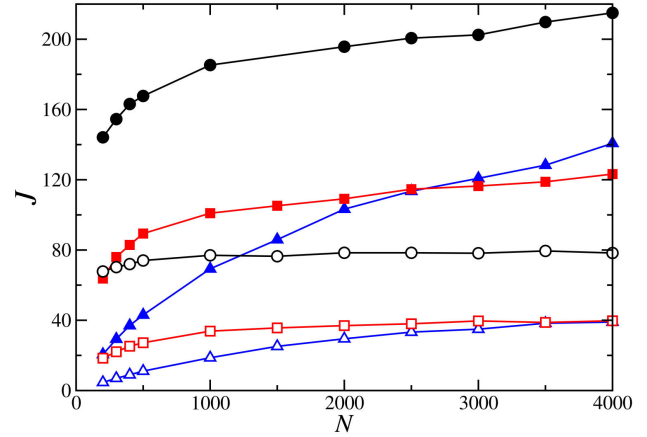


FIGURE 4. (Color online) Heat flux  $J_{\pm}$  vs system size for  $T_+ = 30$  y  $T_- = 5$ . Same  $\alpha$  and  $\beta$  values as in previous figures. Solid symbols correspond to  $J_+$  and void ones to  $J_-$  for the homogeneous, unitary-mass (circles), mass-gradient (squares), and dissimilar-mass (triangles) instances.

The above results seem to indicate that an adequate mass asymmetry can improve rectification figures significantly; however, it is also important to verify how this phenomenology is modified for larger systems sizes. In Fig. 4 we display the behavior of heat fluxes  $J_+$  and  $J_-$  as a function of the lattice size  $N$  for all considered mass distributions. It is readily seen that the magnitude of both heat fluxes for the inhomogeneous-mass cases is lower than that of the corresponding homogeneous counterparts. In the case of the linear mass distribution saturation in the flux values seems to be attained for  $N \sim 1500$ , being largely constant for larger system sizes. A more interesting behavior is displayed by the lattice with dissimilar-mass segments. For  $N < 2000$  the magnitudes of both  $J_+$  and  $J_-$  are markedly inferior not only to those of the homogeneous case, but also to those of the mass-graded lattice. However, it is also noticed that the magnitude of the heat flux  $J_+$  increases rapidly, and for  $N > 2500$  it is greater than that of the homogeneous-mass lattice. Furthermore, its behavior seems to indicate that  $J_+$  will continue to increase for higher  $N$  values than those reported. Therefore, it is expected that the lattice with this type of mass distribution will present the highest rectification efficiency.

In Fig. 5 we report the behavior of the rectification  $r$  as a function of the system size  $N$  for all considered mass distributions. Although the magnitude of the heat fluxes for the instances with inhomogeneous mass distributions are lower than those of the homogeneous-mass case, rectification is higher for the former ones compared to the latter one. In the case of the mass-graded lattice it can be observed in Fig. 4 that the increase rate of  $J_-$  for  $N < 1000$  is sufficient to render a rectification decreases, as seen in Fig. 5; for higher  $N$  values both fluxes are only weakly dependent on system size, and therefore  $r$  remains largely constant. In the case of the lattice with dissimilar masses in both segments  $J_+$  and  $J_-$  increase in the whole range of system sizes studied. For system size values of  $N < 1500$  rectification decreases, as

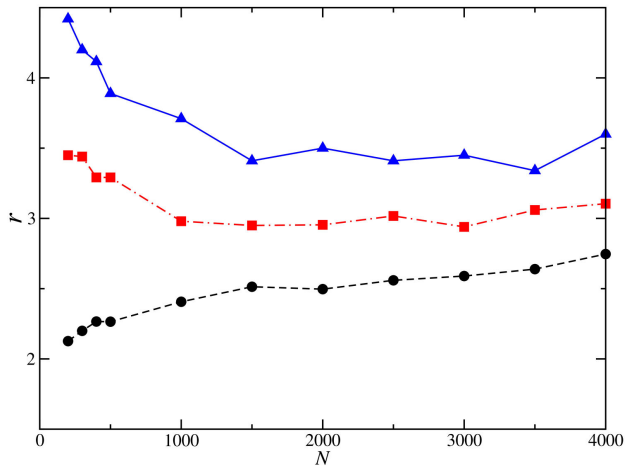


FIGURA 5. (Color online) Thermal rectification  $r$  vs system size  $N$ . Same  $T_+$ ,  $T_-$ ,  $\alpha$ , and  $\beta$  values as in previous figure. The displayed curves correspond to homogeneous, (circles), mass-gradient (squares), and dissimilar-mass (triangles) distributions.

in the previous case. In the range  $1500 < N < 3500$   $J_-$  slowly reaches its saturation value as  $J_+$  keeps increasing; the combined effect of this behavior is that  $r$  fluctuates around a well defined mean, which is the highest one of all considered cases. Finally, for  $N > 3500$  we notice that  $J_-$  seems to attain a saturation value, but not  $J_+$ . Thus rectification  $r$  again increases for  $N = 4000$ . It is highly probable that this behavior will continue for even higher  $N$  values, but further simulations would be necessary to corroborate if it is indeed the case.

#### 4. discussion and conclusions

The physical models employed in the present work, despite their simplicity, are capable to describe a variety of effects of different physical origin. In particular, the FK model, due to the assumptions of the harmonic interatomic force and a sinusoidal on-site (substrate) potential, has the surprising capability to describe a broad spectrum of nonlinear, physically important phenomena, such as propagation of charge-density waves, the dynamics of adsorbed atoms on crystal surfaces, commensurate-incommensurate phase transitions, and domain walls in magnetically ordered structures, among others [26]. On the other hand, the  $\Phi^4$  model, which stems from a discretized Klein-Gordon equation, exhibits generic solutions—discrete breathers—, being time-periodic and (typically exponentially) localized excitations which have been detected, and used for the ensuing theoretical modeling, in Josephson junction networks, arrays of coupled nonlinear optical waveguides, Bose-Einstein condensates loaded on optical lattices, antiferromagnetic layered structures, PtCl based single crystals and driven micromechanical cantilever arrays [27]. Thus the models employed in the present work have an intrinsic physical interest and their study is justified. Now, a mass-graded lattice can be considered as a particular example of a kind of inhomogeneous materials known

as functionally graded materials (FGMs) whose composition and/or structure change gradually in space, which results in corresponding changes in electric, mechanical, thermal, and optical properties. Significantly, such FGMs, *i.e.* nonuniform gradient-mass systems, can be met in nature [28] and can be also purposely manufactured by chemical deposition as well as diffusing techniques [29]. Note also that the optical properties of systems with graded dielectric permittivity match those of gradient-mass systems [30]. Nevertheless, thermal properties of graded materials have not yet been fully studied; our work contributes to fill this gap in our understanding of their behavior. In Ref. 16 significant rectification efficiency was obtained in the large system size limit based in the macroscopic thermal conductivity of two coupled materials. The experimental work inspired by this proposal seems to date the most promising way to design a thermal rectifier of macroscopic size. Therefore it is natural to explore the possibility of modifying the mass distribution of the model proposed in Ref. 16 with an asymmetric mass distribution much closer to that employed in the experiment reported in Ref. 19 in order to obtain further increments in the rectification efficiency. The results presented in Fig. 3 show that such increment is indeed obtained, with a stronger exponential dependence of  $r$  on  $\Delta T$  than that obtained with the linear mass profile. Therefore both mechanisms contribute to a significant increase in the rectification efficiency of our system. Furthermore, we have provided evidence that a much easily obtainable mass distribution can increase the rectification efficiency compared to the graded-mass distribution, being this latter one more difficult to obtain experimentally. Thus our work offers a guide to experimentalists by showing that the simplest mass distribution may indeed be the most adequate to explore the rectification efficiency of a given sample. Finally, since the development of mass-graded structures is technologically anything but a simple problem [1], a search for its realization is being pursued in various alternate directions. Analytically it has been demonstrated that the heat flow in a harmonic mass-graded chain depends only on the boundary masses and the maximum mass in the lattice [31]. It has also been proposed to use silicon filaments together with asymmetrically doped contacts [32]. In place of a spatially varying mass, the idea was also advanced of subjecting a nanotube to nonuniform tension [33], which is equivalent to variation of mass [34,35]. Also, one could apparently employ for this purpose nanodiamond-decorated CNs [36].

The behavior of the positive and negative heat fluxes as a function of the system size shows that, for both mass-asymmetries, the values of  $J_+$  and  $J_-$  are lower than those corresponding to the homogeneous case for all considered  $N$  values, as observed in Fig. 4. This result is consistent with that recently reported for a nearest-neighbor anharmonic oscillator lattice with a mass-gradient, wherein a similar decrease was observed [23]. For large system size values  $r$  seems to approach a saturation value, just as in the homogeneous-mass case, see Fig. 5, but of higher value. However, the most promising result comes from the

dissimilar-mass lattice, wherein the difference  $J_+ - J_-$  increases as  $N$  does so. Furthermore, there seems to be evidence that rectification will attain its ideal limit at macroscopic sizes, although further simulations are needed to corroborate this assumption. It is important to recall that there is evidence that arbitrarily large rectification figures can be obtained with a chaotic billiard chain with noninteracting charged particles in the presence of nonuniform transverse magnetic field, but only for sufficiently small temperature of one of the reservoirs and in the small system size limit [37].

We mention that other structural modifications on systems presenting thermal rectification that may affect their efficiency have also been explored. For example, by means of molecular dynamics simulations of a single-walled CN with randomly located defects only along half the length revealed asymmetric heat conduction at room temperature [38]. The increased overlapping of the phonon density of states when heat flows from the defective part to the pristine one and the intermediate-frequency phonons are mainly responsible for the rectification observed in this system. However, in a system composed of asymmetrically mass-loaded graphene flakes, being these a single layer of carbon atoms in a honeycomb lattice with  $sp^2$  bonds —thus having structure and ther-

mal properties similar to those of CNs—, it was found that that the mass interface between the two regions greatly decreased the thermal conductivity, but did not bring about a thermal rectification effect [39]. This result was explained by the interfacial scattering of solitons in graphene, which revealed a direction-independent energy reflection rate. Thus it is shown that structural differences between two systems can dramatically affect their rectification efficiency, even though the same rectification mechanism, *i.e.* mass-loading, is employed.

In summary, we have proposed two possible structural modifications to a thermal rectifying device composed of two coupled anharmonic lattices that is known to work in the large system size limit. The first one renders a modest increase in rectification power, whereas the second improves it substantially at a fixed size. We also provided evidence that these results may hold for large system sizes.

## Acknowledgments

M. R. B. gratefully acknowledges CONACyT, México and F. T. M. to “Programa Institucional de Formación de Investigadores” I.P.N., México for financial support.

1. N. A. Roberts and D. G. Walker, *Int. J. Therm. Sci.* **50** (2011) 648.
2. C. Starr, *J. Appl. Phys.* **7** (1936) 15.
3. M. Terraneo, M. Peyrard, and G. Casati, *Phys. Rev. Lett.* **88** (2002) 094302.
4. B. Li, L. Wang, and G. Casati, *Phys. Rev. Lett.* **93** (2004) 184301.
5. B. Li, J. Lan, and L. Wang, *Phys. Rev. Lett.* **95** (2005) 104302.
6. N. Li *et al.*, *Rev. Mod. Phys.* **84** 1045 (2011).
7. B. Li, L. Wang, and G. Casati, *Appl. Phys. Lett.* **88** (2006) 143501.
8. L. Wang and B. Li, *Phys. Rev. Lett.* **99** (2007) 177208.
9. L. Wang and B. Li, *Phys. Rev. Lett.* **101** (2008) 267203.
10. E. Pop, *Nano. Res.* **3** (2010) 147.
11. B. Hu and L. Yang, *Chaos* **15** (2005) 015119.
12. B. Hu, L. Yang, and Y. Zhang, *Phys. Rev. Lett.* **97** (2006) 124302.
13. B. Hu, D. He, L. Yang, and Y. Zhang, *Phys. Rev. E* **74** (2006) 060101.
14. E. T. Swartz and R. O. Phol, *Rev. Mod. Phys.* **61** (1989) 605.
15. M. Peyrard, *Europhys. Lett.* **76** (2006) 49.
16. B. Hu, D. He, L. Yang, and Y. Zhang, *Phys. Rev. E* **74** (2006) 060201(R).
17. W. Kobayashi, Y. Teraoka, and I. Terasaki, *Appl. Phys. Lett.* **95** (2009) 171905.
18. T. Takeuchi *et al.*, *J. Appl. Phys.* **111** (2012) 093517.
19. C. W. Chang, D. Okawa, A. Majumdar, and A. Zettl, *Science* **314** (2006) 1121.
20. N. Yang, N. Li, L. Wang, and B. Li, *Phys. Rev. B* **76** (2007) 020301.
21. T. N. Shah and P. N. Gajjar, *Phys. Lett. A* **376** (2012) 438.
22. M. Romero-Bastida and J. M. Arizmendi-Carvajal, *J. Phys. A: Math. Theor.* **46** (2013) 115006.
23. M. Romero-Bastida and A. González-Alarcón, *Phys. Rev. E* **90** (2014) 052152.
24. Z. Rieder, J. L. Lebowitz, and E. Lieb, *J. Math. Phys.* **8** (1967) 1073.
25. F. Thalmann and J. Farago, *J. Chem. Phys.* **127** (2007) 124109.
26. O. M. Braun and Y. S. Kivshar, *Phys. Rep.* **306** (1998) 1.
27. S. Flach and A. V. Gorbach, *Phys. Rep.* **467** (2008) 1.
28. L.-H. He *et al.*, *Act. Biomater.* **9** (2013) 6330.
29. J. P. Huang and K. W. Yu, *Phys. Rep.* **431** (2006) 87.
30. E.-B. Wei, G. Q. Gu, Y. M. Poon, and F. G. Shin, *J. Appl. Phys.* **102** (2007) 074102.
31. K. V. Reich, *Phys. Rev. E* **87** (2013) 052109.
32. P. E. Hopkins and J. R. Serrano, *Phys. Rev. B* **80** (2009) 201408.
33. J. J. Xiao, K. Yakubo, and K. W. Yu, *Phys. Rev. B* **73** (2006) 054201.
34. P. J. Michalski, N. Sai, and E. J. Mele, *Phys. Rev. B* **95**, (2005) 116803.

35. P. J. Michalski and E. J. Mele, *Phys. Rev. B* **76** (2007) 205419.
36. A. Vul' *et al.*, *Adv. Sci. Lett.* **3** (2010) 110.
37. G. Casati, C. Mejía-Monasterio, and T. Prosen, *Phys. Rev. Lett.* **98** (2007) 104302.
38. K. Takahashi, M. Inoue, and Y. Ito, *J. Appl. Phys. Lett.* **49**, (2010) 02BD12.
39. J. Cheh and H. Zhao, *J. Stat. Mech.* **10** (2011) P10031.